Eindhoven University of Technology

BACHELOR

Analysis of a generalised local-density approximation in density-functional theory

Venderbosch, Rogier

Award date:
2022

Department of Mathematics & Computer Science

Analysis of a generalised local-density approximation in density-functional theory

2WH40 Bachelor Final project

R.C. Venderbosch, 1367544

July 9, 2022

Supervisors:
Dr. Björn Baumeier
Ir. W.L.J. Scharpach

Abstract

In this thesis, density-functional theory (DFT) is discussed and implemented using numerical methods. The Kohn–Sham equations are solved for the standard local-density approximation (LDA), which is based on the homogeneous electron gas exchange-correlation energy. The resulting ground state energies of atoms up till and including Neon (atomic number $Z = 10$) are calculated. The calculated ground state energies are typically within 2% above the experimental and theoretically known ground state energies, apart from Hydrogen, where the erroneous self-interaction is most apparent. Next, a generalisation of the local-density approach is analysed, in terms of the parameter q, where $q = 4/3$ is equivalent with standard LDA. The resulting Kohn–Sham equations converge to the Hartree equations for $q \downarrow 1$ and $q \to \infty$, apart from a constant in the first limit. In between these limits we have DFT with exchange energy functional. It is investigated what value of q leads to an optimal prediction of the ground state energy, where optimal means equivalent to the theoretically or experimentally known values. For numerical purposes, we want to be close to the theoretical optimum. For larger atomic numbers, the q-value that for which the optimal ground state energy is achieved seem to converge to 4/3. It is also checked whether the ionisation energy prediction and the total energy prediction can be optimal at the same time. There is a trade-off between the accuracy for the total energy and the ionisation energy. By decreasing q starting from $q = 4/3$, such that the total energy prediction decreases by 1% with respect to the optimal total energy, the ionisation energy prediction can get significantly closer to experimentally known values by at least 10%. No q-value is found for which both the ionisation and total energy are optimal. With this framework the performance of different correlation potentials can be compared in a measure as the distance to the optimum.

Contents

Chapter 1

Introduction

Many processes in your cells depend on electron transfer, without this no biology or life would exist. Electrons are the reason for radiation, which is useful in everyday life in the form of light and enables us to create many advanced technologies, for instance semi-conductors. The stability of atoms and their binding energy is also determined by the electronic structure. Especially the outer electrons are essential in chemistry, there the binding strength of the electrons in atoms or molecules determines many of the material properties. Basically, electrons are everywhere. That is why it is very important to have a good understanding of the electronic structure. The objective for me is to accurately determine ground states and the influence of exchange interactions on this. The ground state is a minimal energy configuration of a given molecule or atom. To get insight in the electron distribution of the atoms, we must refer to electronic structure theory. We will introduce a mathematical method known as *density-functional theory*, it is developed by Kohn and Sham in 1964. The main idea on which this theory was build is that the total of all electrons behaves like a glue, or mush, and not as independent electrons. In 1998, the Nobel Prize in Chemistry was divided between Walter Kohn for his development of density-functional theory and John A. Pople for his development of computational methods. This method is very popular as it has a good balance between accuracy and computational cost. A conclusion of the results is given in Chapter 5.

In Chapter 2, we start with an introduction to electronic structure theory, the theory of atoms and molecules. Our focus will be on atoms, for which several approximation methods are introduced based on the electron density. The approximation that we study is density-functional theory (DFT) where the exchange-correlation is described by the *local-density approximation* (LDA), here the exchange energy of a *homogeneous electron gas* is used to describe an inhomogeneous system. DFT is based on the fact that all properties of a many-particle system can be deduced as a functional of the ground state density and is used to determine the ground state of many-particle systems, in our case atoms. The ground state is the minimal energy state for the particles. After the necessary theory has been established, in Chapter 3 it is applied to a numerical algorithm that solves the eigenfunctions and eigenenergies of an atomic system using the LDA formalism. The main goal will be to analyse the physical properties and accuracy of the LDA algorithm for a generalised exchange-term. The results for the LDA ground state atoms are given in Chapter 4 and serve as a check for the numerical method. After that a generalised form of the exchange-potential is analysed, which is named LDAq. We investigate the total energy, ionisation energy as well as the wave functions themselves. This is done for two limiting cases of the value q and an intermediate regime.

Chapter 2

Electronic structure theory

Solving the time-independent Schrödinger equation for a molecular system is not trivial. An exact solution exists only for Hydrogen consisting of one electron and one proton. For a general molecule, which of a collection of atoms and electrons, approximations are necessary to obtain answers. We start by introducing the Hamiltonian for a general molecule. After that, several approximations will be introduced in order to arrive at a solution. These include the *Born–Oppenheimer* approximation, where the wave functions of the atomic nuclei and electrons are separated. Because the mass of the electrons is much smaller than the nucleur mass, this only induces a relatively small error. After that, the *Hartree–Fock method* and *density-functional theory* is discussed. Both methods rely on the variational principle using functional derivatives to obtain ground state energies.

2.1 Electronic structure theory

We define the Hamiltonian operator for a molecule with M nuclei, each with atomic number Z_α and mass M_α and $\alpha \in \{1, ..., M\}$, together with N electrons as [1]:

$$\begin{aligned} H = &- \sum_{\alpha=1}^{M} \frac{\hbar^2}{2M_\alpha} \nabla_\alpha^2 - \sum_{i=1}^{N} \frac{\hbar^2}{2m_e} \nabla_i^2 - \sum_{i=1}^{N} \sum_{\alpha=1}^{M} \left(\frac{e^2}{4\pi\epsilon_0} \right) \frac{Z_\alpha}{|\mathbf{r}_i - \mathbf{R}_\alpha|} \\ &+ \sum_{\alpha<\beta} \left(\frac{e^2}{4\pi\epsilon_0} \right) \frac{Z_\alpha Z_\beta}{|\mathbf{R}_\beta - \mathbf{R}_\alpha|} + \sum_{i<j} \left(\frac{e^2}{4\pi\epsilon_0} \right) \frac{1}{|\mathbf{r}_i - \mathbf{r}_j|}, \end{aligned} \tag{2.1}$$

where $\hbar$ is the reduced Planck's constant. A brief introduction of the Schrödinger equation is given in Appendix A. The mass of the electron is given by the constant m_e and the elementary charge unit e represents the charge of a single proton; the charge of a single electron is $-e$. The constant ϵ_0 is the vacuum permittivity. The coordinates of the i-th electron are given by $\mathbf{r}_i \in \mathbb{R}^3$ for $i \in \{1, ..., N\}$, similarly $\mathbf{R}_\alpha \in \mathbb{R}^3$ denotes the position of the α-th nucleus. It is beneficial to rewrite (2.1) using *Hartree units*, where we set $m_e = \hbar = e = \frac{1}{4\pi\epsilon_0} = 1$. Using this (2.1) simplifies to:

$$H = T_\mathrm{nuc} + T_\mathrm{el} + V_\mathrm{el,nuc} + V_\mathrm{nuc,nuc} + V_\mathrm{el,el}, \tag{2.2}$$

where the individual terms are defined as

$$T_{\text{nuc}} = -\sum_{\alpha=1}^{M} \frac{1}{2M_\alpha} \nabla_\alpha^2, \tag{2.3}$$

$$T_{\text{el}} = -\sum_{i=1}^{N} \frac{1}{2} \nabla_i^2, \tag{2.4}$$

$$V_{\text{el,nuc}} = -\sum_{i=1}^{N} \sum_{\alpha=1}^{M} \frac{Z_\alpha}{|\mathbf{R}_\alpha - \mathbf{r}_i|}, \tag{2.5}$$

$$V_{\text{nuc,nuc}} = \sum_{\alpha<\beta} \frac{Z_\alpha Z_\beta}{|\mathbf{R}_\alpha - \mathbf{R}_\beta|}, \tag{2.6}$$

$$V_{\text{el,el}} = \sum_{i<j} \frac{1}{|\mathbf{r}_i - \mathbf{r}_j|}. \tag{2.7}$$

$$\tag{2.8}$$

The expression (2.3) denotes the kinetic energy of all the nuclei. Similarly, expression (2.4) denotes the kinetic energy of all the electrons. Expressions (2.5), (2.6) and (2.7) describe the electron-nucleus attraction, nucleus-nucleus repulsion and electron-electron repulsion respectively. The mechanism for the last three terms is the Coulomb interaction between charged particles. The interaction between similar charged particles is repulsive, oppositely charges particles have an attractive interaction.

2.2 The Born–Oppenheimer approximation

Solving the time-independent Schrödinger equation with the Hamiltonian given by (2.2) is a difficult task. A solution would be of the form $\Psi(\underline{\mathbf{R}}, \underline{\mathbf{r}}) \in L^2(\mathbb{R}^{3(M+N)})$, with $\underline{\mathbf{R}} = (\mathbf{R}_1, ..., \mathbf{R}_M) \in \mathbb{R}^{3M}$ and $\underline{\mathbf{r}} = (\mathbf{r}_1, ..., \mathbf{r}_N) \in \mathbb{R}^{3N}$ and depends on all the spatial degrees of freedom of all the individual nuclei and electrons. The Born–Oppenheimer approximation is based on the fact that the nucleur mass is at least an order 10^3 times larger than the electron mass [2]. Due to their larger mass, the nuclei have a much higher inertia and therefore adapt slowly to the motion of their surroundings. However, the electrons adapt (almost) immediately, so that in the reference frame of the electrons, the nuclei can be regarded as immobile. This is the starting point of the Born–Oppenheimer approximation. We assume the total wave function $\Psi(\underline{\mathbf{R}}, \underline{\mathbf{r}})$ can be split in a function describing the nucleur wave function $\Psi_{\text{nuc}}(\underline{\mathbf{r}})$ and an electronic wave function $\Psi_{\text{el}}(\mathbf{r}; \underline{\mathbf{R}})$:

$$\Psi(\underline{\mathbf{R}}, \underline{\mathbf{r}}) = \Psi_{\text{nuc}}(\underline{\mathbf{r}})\Psi_{\text{el}}(\underline{\mathbf{r}}; \underline{\mathbf{R}}). \tag{2.9}$$

The semi-colon is there to stress that the electronic wave function depends parametrically on $\underline{\mathbf{R}}$. The parametric dependence is assumed because the electrons adapt immediately to the motion of the nuclei. With this Ansatz (2.9), the electronic wave function satisfies the *clamped nuclei Schrödinger equation*, which reads

$$\left[T_{\text{el}} + V_{\text{el,nuc}}(\underline{\mathbf{r}}; \underline{\mathbf{R}}) + V_{\text{el,el}}(\underline{\mathbf{r}})\right] \Psi_{\text{el}}(\underline{\mathbf{r}}; \underline{\mathbf{R}}) = E_{\text{el}}(\underline{\mathbf{R}})\Psi_{\text{el}}(\underline{\mathbf{r}}; \underline{\mathbf{R}}). \tag{2.10}$$

The left-hand side of (2.10) defines the electronic Hamiltonian $H_{\text{el}}(\underline{\mathbf{r}}; \underline{\mathbf{R}})$:

$$H_{\text{el}}(\underline{\mathbf{r}}, \underline{\mathbf{R}}) = T_{\text{el}} + V_{\text{el,nuc}}(\underline{\mathbf{r}}; \underline{\mathbf{R}}) + V_{\text{el,el}}(\underline{\mathbf{r}}). \tag{2.11}$$

The eigenvalue problem (2.10) must be solved to find the eigenfunctions $\Psi_{\text{el}}(\underline{\mathbf{r}}; \underline{\mathbf{R}})$ and the eigenvalues $E_{\text{el}}(\underline{\mathbf{R}}) \in \mathbb{R}^{3M}$. Here, the nuclei are not coupled with the dynamics of the electrons due to the parametric dependence. This makes that the eigenvalues depend on the coordinates of all the nuclei positions. On top of this, we also assume that the electrons are in the ground state. That is, they occupy the lowest eigenvalue $E_{\mathrm{el}}(\underline{\mathbf{R}})$ for a given $\underline{\mathbf{R}}$, which we denote by $E^0_{\mathrm{el}}(\underline{\mathbf{R}})$. Therefore, we define

$$E^{\mathrm{eff}}_{\mathrm{el}}(\underline{\mathbf{R}}) := E^0_{\mathrm{el}}(\underline{\mathbf{R}}). \tag{2.12}$$

The function $E^{\mathrm{eff}}_{\mathrm{el}}(\underline{\mathbf{R}})$ is the *effective electronic field* in which the nuclei move. Note that it does not depends on the positions of the electrons. The effective electronic field is considered the potential energy of the nuclear motion. With this, the *nuclear Schrödinger equation*, which is obeyed by the wave function $\Psi_{\mathrm{nuc}}(\mathbf{r})$ reads

$$\left[T_{\mathrm{nuc}} + V_{\mathrm{nuc,nuc}}(\underline{\mathbf{R}}) + E_{\mathrm{el}}(\underline{\mathbf{R}})\right] \Psi_{\mathrm{nuc}}(\underline{\mathbf{r}}) = E_{\mathrm{nuc}} \Psi_{\mathrm{nuc}}(\underline{\mathbf{r}}). \tag{2.13}$$

The nucleur Hamiltonian in (2.13) consists of the kinetic energy of the nuclei and an *effective potential*, which we describe by

$$V^{\mathrm{eff}}_{\mathrm{nuc}}(\mathbf{R}) = V_{\mathrm{nuc,nuc}}(\mathbf{R}) + E^{\mathrm{eff}}_{\mathrm{el}}(\mathbf{R}). \tag{2.14}$$

The nuclear wave function $\Psi_{\mathrm{nuc}}(\underline{\mathbf{r}})$ as well as the nuclear eigenenergy $E_{\mathrm{nuc}} \in \mathbb{R}$ can be solved from the nuclear Schrödinger equation. In the remainder of this chapter, we introduce additional approximation methods known as Hatree–Fock theory and density-functional theory (DFT) to arrive at solutions of the Schrödinger equation with solely the electronic Hamiltonian (2.11). We will be working with atoms consisting of a single nucleus, such that there is no nucleus-nucleus repulsion and fix the position of this nucleus at the origin. In the reference frame of the electrons, the parametric dependence on the nucleus position can be removed. From now on, we thus solve (2.10) and drop the electron subscript el as well as the $\underline{\mathbf{R}}$ dependence. The atomic we consider is described by the atomic number Z.

2.3 Hartree–Fock theory

Using the Born–Oppenheimer approximation, it is still difficult to solve the Schrödinger equation and find the wave function $\Psi(\mathbf{r}_1, ..., \mathbf{r}_N)$ with $\mathbf{r}_i \in \mathbb{R}^3$ for $i \in \{1, ..., N\}$ from the electronic Hamiltonian presented in (2.10). That is because the electrons are correlated. In 1927, Hartree proposed an approximation known as the *Hartree product*, where for N electrons the wave function is given by a product of N single-electron orbitals $\phi_i \in L^2(\mathbb{R}^3)$ for $i \in \{1, ..., N\}$[3] :

$$\Psi(\mathbf{r}_1, ..., \mathbf{r}_N) = \prod_{i=1}^{N} \phi_i(\mathbf{r}_i). \tag{2.15}$$

The imposed condition on the single-electron orbitals is that they are mutually orthonormal, i.e.:

$$\int_{\mathbb{R}^3} \mathrm{d}\mathbf{r} \phi_i^*(\mathbf{r}) \phi_j(\mathbf{r}) = \delta_{ij}. \tag{2.16}$$

This orthonormalility can be used to make the expectation values we will calculate easier, as some term lead to a zero contribution. The wave function (2.15) does, however, not agree with antisymmetrization of the electrons. To incorporate this, we permute all the orbital labels by introducing a permutation $p \in S_N$. The symmetric group S_N consists of all the permutations on the set $\{1, ..., N\}$. Let $\tau(p)$ be the number of pair exchanges needed for the permutation. The sign of the permutation can then be expressed as $\mathrm{sgn}(p) = (-1)^{\tau(p)}$. A linear combination of Hartree products can be combined to form a wave function that is antisymmetric and may be written as

$$\Psi(\mathbf{r}_1, ..., \mathbf{r}_N) = \frac{1}{\sqrt{N!}} \sum_{p \in S_n} (-1)^{\tau(p)} \phi_{p(1)}(\mathbf{r}_1) \dots \phi_{p(N)}(\mathbf{r}_N), \tag{2.17}$$

where the factor $1/\sqrt{N!}$ takes care of the normalisation. Expression (2.17) is equal to writing the wave function in a *Slater determinant.* To simplify the Hamiltonian (2.11), we use the shorthand notation $r_i = |\mathbf{r}_i|$ introduce the single-electron operator h_i for $i \in \{1, ..., N\}$ as:

$$h_i = -\frac{1}{2}\nabla_i^2 - \frac{Z_1}{r_i}. \tag{2.18}$$

By using the operators $h_i := h_i(\mathbf{r}_i)$, which do commute due to absence of the electron-electron interaction, the Hamiltonian (2.11) becomes

$$H = \sum_{i=1}^{N} h_i + \sum_{i<j} \frac{1}{r_{ij}}. \tag{2.19}$$

In order to find the single-electron orbitals, we employ the variational principle [4]. The Hartree–Fock energy E_{HF} is calculated by the expectation value of the Hamiltonian expressed in (2.19)

$$E_{\text{HF}} = \langle \Psi | H | \Psi \rangle = \sum_{i=1}^{N} \langle \Psi | h_i | \Psi \rangle + \sum_{i<j} \langle \Psi | \frac{1}{r_{ij}} | \Psi \rangle . \tag{2.20}$$

We compute both contributions in (2.20) to the energy separately by filling in the Hartree ansatz (2.17). Given some $i \in \{1, ..., N\}$ and $p, p' \in S_N$, the expectation value $\langle \Psi | h_i | \Psi \rangle$ consists of $(N!)^2$ terms ($N!$ being the order of the symmetric group S_N), which all have the same shape

$$\frac{1}{N!}(-1)^{\tau(p)+\tau(p')} \langle \phi_{p(1)}(\mathbf{r}_1) \dots \phi_{p(N)}(\mathbf{r}_N) | \, h_i \, | \phi_{p'(1)}(\mathbf{r}_1) \dots \phi_{p'(N)}(\mathbf{r}_N) \rangle . \tag{2.21}$$

Note that the operator h_i works on $\mathbf{r}_i$. A non-zero value appears only when both permutations are exactly the same. If the permutations are slightly different, the result will be zero due to orthonomality. If both permutations are the same, $(-1)^{\tau(p)+\tau(p')} = (-1)^{2\tau(p)} = 1$. Given that $p(k) = p'(k)$ for all $k \in \{1, ..., N\}$, suppose that $p(i) = p'(i) = j$ for some $i, j \in \{1, ..., N\}$. Then (2.21) reduces to

$$\frac{1}{N!} \langle \phi_j(\mathbf{r}_i) | h_i | \phi_j(\mathbf{r}_i) \rangle . \tag{2.22}$$

Note that we need to take into account all options for $j \in \{1, ..., N\}$, which can by summing over j in (2.22). To account for the degrees of freedom of permutation $p = p'$ where only $p(i) = p'(i) = j$ is fixed, we incorporate another $(N-1)!$ contributions; the size of the permutation group S_{N-1}. Combining the arguments above, we calculate:

$$\sum_{i=1}^{N} \langle \Psi | h_i | \Psi \rangle = \sum_{i=1}^{N} (N-1)! \sum_{j=1}^{N} \frac{1}{N!} \langle \phi_j(\mathbf{r}_i) | h_i | \phi_j(\mathbf{r}_i) \rangle . \tag{2.23}$$

There is no $\mathbf{r}_i$ dependence inside the sum (2.23) anymore , where an integration over $\mathbf{r}_i$ is performed. Therefore, the sum over i evaluates to N. The factorials cancel and expression (2.23) evaluates to

$$\sum_{i=1}^{N} \langle \Psi | h_i | \Psi \rangle = \sum_{j=1}^{N} \langle \phi_j(\mathbf{r}_i) | h_i | \phi_j(\mathbf{r}_i) \rangle . \tag{2.24}$$

By reproducing similar arguments, the second term of (2.20) can be evaluated. Here, the first case where $p = p'$ again leads to a non-zero contribution, but a second possibility exists as well when p and p' differ for two values. For example when $p(i) = p'(j)$ and $p(j) = p'(i)$ and for all $k \in \{1, ..., N\} \setminus \{i, j\}$: $p(k) = p'(k)$. The operator $\frac{1}{r_{ij}}$ works on both $\mathbf{r}_i$ and $\mathbf{r}_j$, so the integral does not vanish. The first case covers an expression for the Coulomb energy of the interacting electrons, the second case an exchange energy. Combining results with (2.24), the total energy functional for the antisymmetrized Hartree wave function is

$$\begin{aligned} E_{\mathrm{HF}} =& \sum_{j=1}^{N} \langle \phi_j(\mathbf{r}_i) | h_i | \phi_j(\mathbf{r}_i) \rangle \\ &+ \frac{1}{2} \sum_{i=1}^{N} \sum_{j=1}^{N} \left(\langle \phi_i(\mathbf{r}_j)\phi_j(\mathbf{r}_i) | \frac{1}{r_{ij}} | \phi_i(\mathbf{r}_j)\phi_j(\mathbf{r}_i) \rangle - \langle \phi_i(\mathbf{r}_j)\phi_j(\mathbf{r}_i) | \frac{1}{r_{ij}} | \phi_j(\mathbf{r}_j)\phi_i(\mathbf{r}_i) \rangle \right) . \end{aligned} \tag{2.25}$$

The goal is to minimize $E_{\mathrm{HF}}[\phi_i]$ with respect to $\phi_i^*(\mathbf{r}_i)$ under the constraint that $\langle \phi_i | \phi_j \rangle = \delta_{ij}$ for the obitals to remain orthonormal. The variables $\mathbf{r}_i$ are actually dummy variables and are from now on replaced by $\mathbf{r}$. This variational procedure can be executed by introducing the Lagrange multipliers ϵ_{ij} to satisfy the constraint:

$$\frac{\delta}{\delta \phi_i^*} \left\{ E_{\mathrm{HF}}[\phi_i] - \sum_{i=1}^{N} \sum_{j=1}^{N} \epsilon_{ij} [\langle \phi_i | \phi_j \rangle - \delta_{ij}] \right\} = 0. \tag{2.26}$$

Performing the functional derivative leads to the Hartree–Fock equations:

$$\left[-\frac{1}{2} \nabla^2 - \frac{Z}{r} + \int_{\mathbb{R}^3} d\mathbf{r}' \frac{n(\mathbf{r}')}{|\mathbf{r} - \mathbf{r}'|} \right] \phi_i(\mathbf{r}) - \sum_{j=1}^{N} \int_{\mathbb{R}^3} d\mathbf{r}' \frac{\phi_j^*(\mathbf{r}')\phi_i(\mathbf{r}')}{|\mathbf{r} - \mathbf{r}'|} \phi_j(\mathbf{r}) = \epsilon_i \phi_i(\mathbf{r}), \tag{2.27}$$

$$\rho(\mathbf{r}) = \sum_{i=1}^{N} |\phi_i(\mathbf{r})|^2. \tag{2.28}$$

From the variational method, we yield the Hartree–Fock equations, a system of N coupled equations for the N single-electron orbitals (2.27). These individual eigenfunctions contribute to the electron density via (2.28) and by construction they form a solution for which the total energy is minimized whilst satisfying the antisymmetric property of electrons.

2.4 Density-functional theory

For an atom with N electrons it is necessary to keep track of $3N$ coordinates. Density-functional theory (DFT) is based on a reduction of dimensionality of the original many-body problem, and consists of keeping track of an electron density $\rho(\mathbf{r})$. It turns out that every property of interacting particles can be viewed as a functional of the ground-state density $\rho_0(\mathbf{r})$. The ground-state density is the density that minimizes the energy. The underlying reason for this was established in 1964 by Hohenberg and Kohn and stated in the next theorems.

2.4.1 Hohenberg–Kohn theorems

The Hohenberg–Kohn theorems splits the energy functional in a universally valid functional describing electron-electron interaction and kinetic energy [5]. The system dependent functional is captured in the general external potential $v_{\text{ext}}(\mathbf{r})$.

Theorem 1 (First Hohenberg–Kohn theorem)**.** *The external potential* $v := v_{\text{ext}}(\boldsymbol{r})$ *is a unique functional, up to a constant, of the ground-state electron density* $\rho_0(\boldsymbol{r})$*.*

Proof. The theorem is proven by *reductio ad absurdum.* Assume there is another external potential $v'(\mathbf{r})$ where $(v - v') \neq \text{constant})$ that gives rise to the same ground-state density $\rho_0(\mathbf{r})$. Both potentials belong to distinct Hamiltonians $H'(\mathbf{r})$ and $H(\mathbf{r})$ with distinct wave functions $\psi'(\mathbf{r})$ and $\psi(\mathbf{r})$ and energies E' and E. Using the variational principle,

$$E' = \langle \psi' | H' | \psi' \rangle < \langle \psi | H' | \psi \rangle = \langle \psi | H + v' - v | \psi \rangle \, , \tag{2.29}$$

so that for the energy we find

$$E' < E + \int d\mathbf{r}[v' - v]\rho(\mathbf{r}). \tag{2.30}$$

By changing primed and unprimed, similarly we find that

$$E < E' + \int d\mathbf{r}[v - v']\rho(\mathbf{r}). \tag{2.31}$$

Together this leads to

$$E + E' < E + E', \tag{2.32}$$

which is a contradiction. ☐

From Theorem 1, it follows that the electron density uniquely determines the Hamiltonian operator. This is because the Hamiltonian is specified by the number of electrons and the external potential. The Hamiltonian itself determines the whole system, so that every electronic property can be viewed as a functional of the ground-state density $\rho_0(\mathbf{r})$.

Variation in the universal energy functional $E_v[\rho(\mathbf{r})]$ can be performed and the resulting ground state-energy E_0 is the minimum of the energy functional. A proof follows from the Rayleigh-Ritz principle and is given in [6].

It is worthwhile to notice that the Hohenberg–Kohn theorems do not give an explicit method to obtain the electron ground state. The difficulty is finding $F[\rho]$, which cannot be described by an exact functional in general. Kohn and Sham devised a method for carrying out these calculations that is known as density-functional theory (DFT) and this is described in the next section.

2.4.2 Kohn–Sham formulation

Consider the Hamiltonian for our atomic system (2.11). If we want to use the Hohenberg–Kohn theorems, an expression for the functional $F[\rho]$ is necessary. Given a certain external potential $v_{\text{ext}}(\mathbf{r})$, the energy functional thus can be defined as

$$E[\rho] = T[\rho] + V_{ee}[\rho] + \int_{\mathrm{R}^3} \rho(\mathbf{r})v_{\text{ext}}(\mathbf{r})\text{d}\mathbf{r}. \tag{2.33}$$

In (2.33), the kinetic energy functional $T[\rho]$ and electron-electron functional $V_{ee}[\rho]$ are added to form the universal functional $F[\rho]$. This part is universal as it does not depend on the external potential. The challenge with the energy expression (2.33) is that it is difficult to get an accurate description of the kinetic energy functional $T[\rho]$ for a many-electron system. Instead of solving the problem for interaction particles, Kohn and Sham introduced an system of non-interaction particles which has the same electron density as the real system [7]. Using the single-particle orbitals ϕ_i, the density is described by the sum of single-particle densities:

$$\rho(\mathbf{r}) = \sum_{i=1}^{N} |\phi_i(\mathbf{r})|^2. \tag{2.34}$$

The kinetic energy functional for this non-interacting system can be established as the sum over the expectation value over single particle kinetic energies as

$$T_s[\rho] = \sum_{i=1}^{N} \int_{\mathbb{R}^3} \text{d}\mathbf{r}\phi_i^*(\mathbf{r})(-\frac{1}{2}\nabla^2)\phi_i(\mathbf{r}). \tag{2.35}$$

When the translation from the interaction kinetic energy $T[\rho]$ to the non-interacting energy $T_s[\rho]$ is made, this induces an unknown error. This error $T[\rho] - T_s[\rho]$ and other unknown contributions are put in the exchange-correlation (XC) functional. It describes the exchange energy and correlation energy of the many-electron system, which are purely quantum mechanical effects. The total energy functional is then

$$E[\rho] = T_s[\rho] + \int_{\mathbb{R}^3} \rho(\mathbf{r})v_{\text{ext}}(\mathbf{r})\text{d}\mathbf{r} + \frac{1}{2}\int_{\mathbb{R}^3}\int_{\mathbb{R}^3} \frac{\rho(\mathbf{r})\rho(\mathbf{r}')}{|\mathbf{r}-\mathbf{r}'|}\text{d}\mathbf{r}\text{d}\mathbf{r}' + E_{\text{XC}}[\rho]. \tag{2.36}$$

The third term from (2.36) is the *Hartree energy* also denoted by $E_{\text{H}}[\rho]$, it is the functional for the electron-electron interactions. According to the second Hohenberg–Kohn theorem, the orbitals can be varied so that a ground-state energy is found from the ground-state density, similarly to the Hartree–Fock process. Again, the condition for the single-particle orbitals is that they are orthonormal. The resulting Kohn–Sham equations looks like

$$\left(-\frac{1}{2}\nabla^2 + v_{\text{ext}}(\mathbf{r}) + V_{\text{H}}[\rho](\mathbf{r}) + V_{\text{XC}}[\rho](\mathbf{r})\right)\phi_i(\mathbf{r}) = \epsilon_i\phi_i(\mathbf{r}), \tag{2.37}$$

where

$$V_{\text{XC}}(\mathbf{r}) = \frac{\delta E_{\text{XC}}[\rho]}{\delta\rho}. \tag{2.38}$$

The Kohn–Sham equations are a method, similarly to Hartree–Fock, to reduce a many-electron system to a set of single-electron orbitals. The eigenvalues here do not have a specific meaning as single particle energies because the system itself cannot be simply described as a collection of single particles. These eigenvalues are the Lagrange multipliers to ensure that the total number of electrons is N. Once we have solved the Kohn–Sham equations, the ground state orbitals $\phi_i(\mathbf{r})$ and thereby the density $\rho(\mathbf{r})$ is known. With this, the total energy can be calculated by employing (2.36). To write the total energy in terms of the sum over Kohn–Sham eigenvalues, we multiply (2.37) by $\phi_i^*(\mathbf{r})$ and integrate over $\mathbb{R}^3$. Add up the result for each eigenvalue whilst making use of (2.34) results in

$$\sum_{i=1}^{N}\epsilon_i = \sum_{i=1}^{N}\int_{\mathbb{R}^3}\mathrm{d}\mathbf{r}\phi_i^*(\mathbf{r})(-\frac{1}{2}\nabla^2)\phi_i(\mathbf{r})+\int_{\mathbb{R}^3}\mathrm{d}\mathbf{r}\rho(\mathbf{r})v_{\text{ext}}(\mathbf{r})+\int_{\mathbb{R}^3}\mathrm{d}\mathbf{r}d\mathbf{r}'\frac{\rho(\mathbf{r})\rho(\mathbf{r}')}{|\mathbf{r}-\mathbf{r}'|}+\int_{\mathbb{R}^3}\mathrm{d}\mathbf{r}V_{\text{XC}}(\mathbf{r})\rho(\mathbf{r}). \quad (2.39)$$

By comparing (2.36) with (2.39), the total energy can be written in terms of the Kohn–Sham eigenvalues:

$$E[\rho] = \sum_{i=1}^{N}\epsilon_i - E_H[\rho] + (E_{\text{XC}}[\rho] - V_{\text{XC}}(\mathbf{r})). \quad (2.40)$$

In the Kohn–Sham formulation, an exact solution of an interacting electron system can be found in theory. In practice, this does not work due to the exchange and correlation potential, for which an exact form is not generally known. In certain systems, an exact formulation of the exchange part is known, for example the homogeneous electron gas described in Sec. **??**.

2.4.3 Local-density approximation

The main interest in density-functional theory is to find an accurate description for the exchange-correlation functional, which needs to be approximated by some method. Here, we discuss the local-density approximation or LDA for short, which is widely used in DFT. It is one of the simplest approximations that can be made for the unknown exchange-correlation functional. But it is also remarkably succesful for a wide range of systems delivering high accuracy results [8]. To arrive at LDA, the exchange-correlation potential is often decomposed into the exchange and correlation parts as

$$E_{\text{XC}} = E_{\text{X}} + E_{\text{C}}. \quad (2.41)$$

Both parts can now be treated seperately. Starting with the exchange term, we want to use our knowledge of the homogeneous electron gas to get an approximate expression for the exchange functional. We suppose that *locally* the system has the same exchange energy per electron as the homogeneous electron gas (HEG). The exchange energy of the homogeneous electron gas can be analytically calculated and reads

$$\varepsilon_{\text{x}}(\rho) = -\frac{3}{4}\left(\frac{3\rho}{\pi}\right)^{1/3}. \quad (2.42)$$

This exchange energy per electron is multiplied by the number of electrons in a small volume, which is $\rho(\mathbf{r})\mathrm{d}\mathbf{r}$, and integrated over $\mathbb{R}^3$ to obtain the total exchange energy of the system,

$$E_{\text{X}}[\rho] = \int_{\mathbb{R}^3}\rho(\mathbf{r})\epsilon_{\text{X}}(\rho(\mathbf{r}))\mathrm{d}\mathbf{r}. \quad (2.43)$$

For mathematical purposes [9], we want to investigate a generalisation of (2.43) and (2.42) expressed in terms of the exponent $q \in [1,\infty)$:

$$E_X[\rho] = \frac{\lambda}{q}\int_{\mathbb{R}^3}\rho(\mathbf{r})^q\mathrm{d}\mathbf{r}, \quad (2.44)$$

$$V_X(\rho(\mathbf{r})) = \lambda\rho(\mathbf{r})^{q-1}. \quad (2.45)$$

Here $\lambda \in \mathbb{R}$ is a constant and for $\lambda = \left(\frac{3}{\pi}\right)^{1/3}$ and $q = 4/3$ we have the same exchange energy as the homogeneous electron gas. From a physical perspective, the exponent $q = \frac{4}{3}$ is thus very interesting.

The correlation energy is not exactly known, several methods exist to approximate it. We will use one of the more popular choices by Vosko–Wilk expressed in the Wigner–Seitz radius [10]. The Wigner–Seitz radius is the radius of a sphere with a volume equal to the volume of an electron. It is a local property related to the local density by

$$\frac{4}{3}\pi r_s^3 = \frac{1}{\rho}. \tag{2.46}$$

Vosko–Wilk have calculated the energy of the homogeneous electron gas for a wide range of densities and used Monte Carlo techniques to get an approximation for the correlation energy:

$$\epsilon_C(r_s) = \frac{A}{2}\left\{\log\left(\frac{x^2}{X(x)}\right) + 2\frac{b}{Q}\operatorname{atan}(\frac{Q}{2x+b}) - \frac{bx_0}{X(x_0)}\left[\log\left(\frac{(x-x_0)^2}{X(x)}\right) + \frac{2(b+2x_0)}{Q}\operatorname{atan}(\frac{Q}{2x+b})\right]\right\}, \tag{2.47}$$

where $x = \sqrt{r_s}$, $X(x) = x^2 + bx + c$ and $Q = \sqrt{4c - b^2}$ with parameters $A = 0.0621814$, $x_0 = -0.10498$, $b = 3.72744$ and $c = 12.9352$. The exchange energy functional is then written analogously to (2.43) as

$$E_{\mathrm{C}}[\rho] = \int_{\mathbb{R}^3} \rho(\mathbf{r})\epsilon_{\mathrm{C}}(\rho(\mathbf{r}))\mathrm{d}\mathbf{r}. \tag{2.48}$$

The correlation potential can be calculated with functional derivatives and equals

$$V_{\mathrm{C}}(r_s) = \frac{\delta E_C[\rho(\mathbf{r})]}{\delta\rho(r)} = \epsilon_c - \frac{1}{6}A\frac{c(x-x_0) - bxx_0}{(x-x_0)(x^2+bx+c)}. \tag{2.49}$$

Together with the exchange potential (2.42), the full exchange-correlation potential inside the Kohn–Sham equations is approximated using LDA. Thereby, all necessary ingredients in order to solve the Kohn–Sham equations are known (approximately). Next, we want to actually start solving the Kohn–Sham equations, for which we use numerical methods in the next chapter.

Chapter 3

Numerical implementation

The Kohn–Sham equations are self-consistent as the Hartree potential (3.21) depends on the electron density, which itself depends on the Hartree potential via the Kohn–Sham equations (2.37). A self-consistent solution is a solution leading to a density, which in turn gives rise to the same potential. A brief overview of the elements necessary to solve such differential equations is given, starting with a numerical method for both the Kohn–Sham equations and the Hartree potential. We let the numerical method work on a logarithmic grid with more points around the origin. Finally the connection between the individual elements is treated giving rise to the correct solution method that we have implemented in Python.

3.1 Numerov's method

In this thesis, we use Numerov's method, which is a numerical stepping method that can be e applied to differential equations of the specific form

$$\frac{\mathrm{d}^2 f(r)}{\mathrm{d}r^2} = g(r)f(r) + s(r). \tag{3.1}$$

We call (3.1) a Numerov type equation and assume that $f \in C^5[0,\infty)$, $g, s \in C^3[0,\infty)$ and $r \in [0,\infty)$. The functions $g(r)$ and $s(r)$ are supposed to be known and we want to solve for $f(r)$. To derive the numerical scheme that belongs to the Numerov-type equation, we expand $f(r \pm h)$ in a Taylor series around $f(r)$ for some $h > 0$:

$$f(r \pm h) = f(r) \pm h\frac{\mathrm{d}f(r)}{\mathrm{d}r} + \frac{h^2}{2}\frac{\mathrm{d}^2 f(r)}{\mathrm{d}r^2} \pm \frac{h^3}{3!}\frac{\mathrm{d}^3 f(r)}{\mathrm{d}r^3} + \frac{h^4}{4!}\frac{\mathrm{d}^4 f(r)}{\mathrm{d}r^4} \pm \frac{h^5}{5!}\frac{d^5 f(r)}{\mathrm{d}r^5} + O(h^6). \tag{3.2}$$

Adding $f(r+h)$ and $f(r-h)$ gives

$$\frac{\mathrm{d}^2 f(r)}{\mathrm{d}r^2} = \frac{f(r+h) - 2f(r) + f(r-h)}{h^2} - \frac{h^2}{12}\frac{\mathrm{d}^4 f(r)}{\mathrm{d}r^4} + O(h^6). \tag{3.3}$$

An expression for the fourth-order derivative in (3.3) can be found by differentiating (3.1) twice:

$$\frac{\mathrm{d}^4 f(r)}{\mathrm{d}r^4} = \frac{\mathrm{d}^2\left(g(r)f(r)\right)}{\mathrm{d}r^2} + \frac{\mathrm{d}^2 s(r)}{\mathrm{d}r^2}. \tag{3.4}$$

The second-order derivatives in (3.4) can be expanded in a similar fashion to obtain:

$$\frac{\mathrm{d}^4 f(r)}{\mathrm{d}r^4} = \frac{f(r+h)g(r+h) - 2f(r)g(r) + f(r-h)g(r-h)}{h^2} + \frac{s(r+h) - 2s(r) + s(r-h)}{h^2}) + O(h^4). \tag{3.5}$$

Expression (3.5) can subsequently be substituted in (3.3), which itself is again substituted in (3.1) to find the numerical scheme. We discretize the variable r into M points to form a linear grid

$$r_m := mh, \tag{3.6}$$

where $m \in \{1, ..., M\}$ and h denotes the step-size. Furthermore, let us define $f_m := f(r_m)$, $g_m := g(r_m)$ and $s_m := s(r_m)$. The numerical scheme then reads [11]

$$\left(1 - \frac{h^2}{12} g_{m+1}\right) f_{m+1} + \left(1 - \frac{h^2}{12} g_{m-1}\right) f_{m-1} - \left(2 + \frac{10h^2}{12} g_m\right) f_m = \frac{h^2}{12}\left(s_{m+1} + 10 s_m + s_{m-1}\right) + O(h^6). \tag{3.7}$$

The derivation that is explained in this section works because the right-hand side of the Numerov-type equation does not depend on the derivative of f. The result is a stepping algorithm that can solve f_i based on the previous two values f_{i-1} and f_{i-2} for $i \in \{3, ..., M\}$, which is sixth-order accurate.

3.2 Logarithmic grid

Numerov's method as introduced in Sec. 3.1 assumes an equal spacing in the grid for the $r-$coordinates. Because of the singularities in the Coulomb interaction close to the origin, the chance for large derivatives is larger in the region of small r. To match this numerically, it is beneficial for the accuracy to increase the number of points close to $r = 0$. For large r, the number of points can be reduced to minimize the computational cost. A logarithmic grid fulfills these properties. It is however non-trivial to apply a logarithmic grid due to the nonuniform spacing. In order to solve (3.1) on a logarithmic grid for $f(r)$, we proceed and show an alternative differential equation defined on a uniform grid. At the end, the solution of the alternative problem is connected to the solution of (3.1) on a logarithmic grid. To find the correct 'alternative problem', let us start by introducing a coordinate transformation from the variable r to a new variable $u \in [0, \infty)$ where we use the following relations throughout this section:

$$r = r(u) = \alpha(e^u - 1) \quad \longleftrightarrow \quad u = u(r) = \ln\Big(\frac{r}{\alpha} + 1\Big), \tag{3.8}$$

with $\alpha \in (0, \infty)$ a constant. We willdefine a uniformly spaced grid in terms of the variable u for $m \in \mathbb{Z}$:

$$u_m := mh. \tag{3.9}$$

This is accompanied by a logarithmic grid r_m^*:

$$r_m^* := \alpha(e^{u_m} - 1). \tag{3.10}$$

Our objective is a function $\tilde{f}(u)$, which can be solved numerically on the uniformly spaced grid u_m, allowing us to use Numerov's method. For that, the differential equation for $\tilde{f}(u)$ must also satisfy the shape of a Numerov-type equation, with yet unknown functions $\tilde{s}(u)$ and $\tilde{g}(u)$. Once $\tilde{f}(u)$ is known, we must translate it to $f(r)$, the solution of (3.1). We define a relation between $f(r)$ and $\tilde{f}(u)$ [12]:

$$f(r) := \alpha e^{u/2}\tilde{f}(u). \tag{3.11}$$

By using the chain rule for second derivatives we have

$$\frac{\mathrm{d}^2 f(r)}{\mathrm{d}r^2} = \frac{\mathrm{d}^2 f(r)}{\mathrm{d}u^2}\left(\frac{\mathrm{d}u}{\mathrm{d}r}\right)^2 + \frac{\mathrm{d}f(r)}{\mathrm{d}u}\frac{\mathrm{d}^2 u}{\mathrm{d}r^2} = \frac{\alpha e^{u/2}}{(r+\alpha)^2}\left(\frac{\mathrm{d}^2\tilde{f}(u)}{\mathrm{d}u^2} - \frac{1}{4}\tilde{f}(u)\right). \tag{3.12}$$

Note that here the terms $\frac{\mathrm{d}\tilde{f}(u)}{\mathrm{d}u}$ cancel out, so that it does not depend on the first derivative and definition (3.11) works. That means it will lead us to a Numerov-type equation. This Numerov-type equation for the function $\tilde{f}(u)$ can be deduced by substitution of (3.11) and (3.12) in (3.1). We find

$$\frac{\mathrm{d}^2\tilde{f}(u)}{\mathrm{d}u^2} = \tilde{g}(u)\tilde{f}(u) + \tilde{s}(u), \tag{3.13}$$

for which the relations for $\tilde{g}(u)$ and $\tilde{s}(u)$ are given by:

$$\tilde{g}(u) = (r+\alpha)^2 g(r) + \frac{1}{4}, \tag{3.14}$$

$$\tilde{s}(u) = \frac{(r+\alpha)^2}{\alpha e^{u/2}} s(r). \tag{3.15}$$

In order to solve the differential equation (3.1) on a logarithmic grid, we perform the following steps:

1. State the Numerov-type equation to be solved with known $g(r)$ and $s(r)$, (3.1);
2. Calculate $\tilde{g}(u)$ and $\tilde{s}(u)$ using (3.14) and (3.15);
3. Solve $\tilde{f}(u_m)$ on the uniform grid u_m with Numerov's method (3.13)
4. Calculate $f(r_m^*)$ from (3.11).

The final result is $f(r_m^*)$ has a logarithmic grid spacing with more points close to the origin.

3.3 Radial Kohn–Sham equations

We want to study the behaviour of atoms via the Kohn–Sham equations (2.37), which we solve numerically. In this case, the general external potential is given by $v_{\text{ext}}(\mathbf{r}) = -\frac{Z}{|\mathbf{r}|}$. For simplicity, let us now introduce the effective potential $V_{\text{eff}}(\mathbf{r})$ for this specific problem as

$$V_{\text{eff}}(\mathbf{r}) = -\frac{Z}{|\mathbf{r}|} + V_{\text{H}}(\mathbf{r}) + V_{\text{XC}}(\mathbf{r}). \tag{3.16}$$

With the same quantum numbers n, l and m (See Appendix A.3) that are used for 3D quantum mechanics, the Kohn–Sham equations (2.37) transform and becomes

$$-\frac{1}{2}\nabla^2\phi_{n,l,m}(\mathbf{r}) + V_{\text{eff}}(\mathbf{r})\phi_{n,l,m}(\mathbf{r}) = \varepsilon_{n,l,m}\phi_{n,l,m}(\mathbf{r}). \tag{3.17}$$

The effective potential is assumed to be spherically symmetric, so that we can write $V_{\text{eff}}(\mathbf{r}) = V_{\text{eff}}(r)$. Due to this spherical symmetry, we adopt spherical coordinates (r, θ, φ) and look for separable solutions of the shape

$$\phi_{n,l,m}(r, \theta, \varphi) = R_{n,l}(r) Y_{l,m}(\theta, \varphi). \tag{3.18}$$

Substitution of (3.18) into (3.17) leads to an angular wave equation for $Y_{l,m}(\theta, \varphi)$ and a radial equation for $R_{n,l}(r)$, Appendix A.3. The potential $V_{\text{eff}}(r)$ only affects the radial equation due to spherical symmetry. Upon introducing $u_{n,l}(r) = rR_{n,l}(r)$, (3.17) becomes

$$-\frac{1}{2}\frac{\mathrm{d}^2 u_{n,l}(r)}{\mathrm{d}r^2} + \left[V_{\text{eff}}(r) + \frac{l(l+1)}{2r^2}\right] = \varepsilon_{n,l} u_{n,l}(r). \tag{3.19}$$

Equation (3.19) is solved numerically with the Numerov algorithm. The total energy functional in spherical coordinates transforms from (2.40) to:

$$E = \sum_{n,l} 2(2l+1)\varepsilon_{n,l} f_{n,l} + \int_{\mathbb{R}} \mathrm{d}r 4\pi r^2 \tilde{\rho}(r) \left[-\frac{1}{2}\frac{U_H(r)}{r} + (E_{\text{xc}} - V_{\text{xc}})\right]. \tag{3.20}$$

The summation over n, l is bounded and determined by the occupation of the electron shells, which depends on the specific atom.

3.4 Poisson equation

The Hartree potential in the Kohn–Sham equations (2.37) is given by:

$$V_{\text{H}}(\mathbf{r}) = \int_{\mathbb{R}^3} \frac{\rho(\mathbf{r}')}{|\mathbf{r} - \mathbf{r}'|} \mathrm{d}\mathbf{r}'. \tag{3.21}$$

Instead of doing the integration, it is more efficient to solve the corresponding differential equation where we make use of the property $\nabla^2 \frac{1}{|\mathbf{r}|} = -4\pi\delta(\mathbf{r})$, this leads to the following differential equation:

$$\nabla^2 V_{\text{H}}(\mathbf{r}) = -4\pi\rho(\mathbf{r}). \tag{3.22}$$

Because of spherical symmetry, this Laplacian reduces to an ordinary 1D derivative because the Hartree potential only depends on the radial coordinate r. Upon introducing $U(r) = V_{\text{H}}(r)r$ and the radial density $\tilde{\rho}(r)$, it becomes:

$$\frac{\mathrm{d}^2 U(r)}{\mathrm{d}r^2} = -4\pi r \tilde{\rho}(r). \tag{3.23}$$

The boundary conditions can be derived from physical arguments. First of all, the potential needs to be finite at $r = 0$, i.e. $V_{\text{H}}(0) < \infty$. This implies that $U(0) = 0$. The second boundary condition can be derived from charge conservation. The total charge N of the electrons is given by the integral

$$N = \int_{\mathbb{R}^3} \rho(\mathbf{r}) \mathrm{d}\mathbf{r}. \tag{3.24}$$

For r large enough all the charge should be confined. This allows us to estimate the distance $\frac{1}{|\mathbf{r}-\mathbf{r}'|}$ in (3.21) by using the cosine law

$$\frac{1}{|\mathbf{r}-\mathbf{r}'|} = \frac{1}{r}\frac{1}{1-|\frac{\mathbf{r}'}{\mathbf{r}}|} = \frac{1}{r}\left(1-2\frac{\mathbf{r}'\cdot\mathbf{r}}{|\mathbf{r}|^2}+\left(\frac{|\mathbf{r}'|}{|\mathbf{r}|}\right)^2\right)^{-1/2} = \frac{1}{r}\frac{1}{\sqrt{1+\varepsilon}}, \tag{3.25}$$

where $\varepsilon = -2\frac{\mathbf{r}'\cdot\mathbf{r}}{|\mathbf{r}|^2}+\left(\frac{|\mathbf{r}'|}{|\mathbf{r}|}\right)^2$. By applying the Binomial series[1] to (3.25), it can be deduced that

$$\frac{1}{|\mathbf{r}-\mathbf{r}'|} = \frac{1}{r}+O\left(\frac{r'}{r^2}\right) \quad \text{as} \quad r\to\infty. \tag{3.26}$$

For this expansion, we have used the relation $\mathbf{r}'\cdot\mathbf{r} \leq |\mathbf{r}'||\mathbf{r}| := r'r$ and used the big-O notation. We write $f(x) = O(g(x))$ as $x\to\infty$ provided that $|f(x)| \leq K|g(x)|$ for all $x \geq x_0$ for some constant $K\in\mathbb{R}^+$ with $x_0\in\mathbb{R}$. The Hartree equation (3.21) can be estimated in the limit $r\to\infty$ employing (3.26):

$$V_{\mathrm{H}}(\mathbf{r}) = \lim_{r\to\infty}\frac{1}{r}\int_{\mathbb{R}^3}\mathrm{d}\mathbf{r}\rho(\mathbf{r}). \tag{3.27}$$

Comparing (3.27) with (3.24), the second boundary condition is determined to be:

$$\lim_{r\to\infty} U(r) = N. \tag{3.28}$$

The boundary condition for numerical purposes is described in terms of the variable $r_{\max}$, which is the maximal value of the radial grid and reads $U(r_{\max}) = N$. In general, $r_{\max}$ should be large enough such that the distance function (3.26) is well described by the first term of the expansion. Also, $r_{\max}$ should be physically large enough in order for it to be reasonable to assume that all charge is confined in 3D space bounded by $r_{\max}$. Due to the self-consistency, the Hartree potential needs to be calculated again upon changing the density until the solution is self-consistent. To do so, we introduce a Poisson solver that works on the same logarithmic grid (3.10) and makes use of the Numerov numerical scheme presented in (3.7). The Numerov integration method, as introduced in Sec. 3.1, calculates the value in the new mesh points from start to end or vice versa. To satisfy both boundary conditions, we solve a different initial value problem $\tilde{U}(r)$ solving the same differential equation (3.23) with different boundary conditions $\tilde{U}(0) = 0$ and $\tilde{U}'(0) = 1$. This is easier for the stepping algorithm, which starts from the origin. These By adding a homogeneous solution of (3.23), the choice of the constant allows us to match the true solution $U(r)$ to the correct boundary condition as expressed by (3.28) together with $U(0) = 0$. The solutions reads

$$U(r) = \tilde{U}(r) + r\frac{N-\tilde{U}(r_{\max})}{r_{\max}}. \tag{3.29}$$

To see why (3.29) is a solution with the correct boundary conditions, we must first remark that it is indeed a solution. This is the case, because $\tilde{U}(r)$ is a solution (3.23) and the second term consists of a constant times r, which evaluates to 0 upon differentiating twice. Filling in $r = 0$, we obtain $U(0) = \tilde{U}(0) = 0$. Filling in $r_{\max}$ results in $U(r) = \tilde{U}(r_{\max}) + N - \tilde{U}(r_{\max}) = N$.

---

[1] Bionomial series: $(1+x)^s = \sum_{n=0}^{\infty}\binom{s}{n}x^n$ [13].

3.5 Self-consistent field

Now that we have a Poisson solver together with a numerical method for the Kohn–Sham equations, the task is to combine this to find ground states. The self-consistent field method is an iterative method where we take an approximate solution of the electron density from which the Hartree and exchange-correlation potential is calculated. From these potentials the new electron density can be calculated via the Kohn–Sham equations and the process repeats itself. To explain the implementation of the *self-consistent field* (SCF) process [14], we rewrite the radial Kohn–Sham equations here as

$$\left(-\frac{1}{2}\nabla^2 + v_{\text{ext}}(r) + V_{\text{H}}[\rho^{\text{in}}(r)](r) + V_{\text{XC}}[\rho^{\text{in}}(r)](r) + \frac{l(l+1)}{2r^2}\right) u_{n,l}(r) = \epsilon_{n,l} u_{n,l}(r), \tag{3.30}$$

$$\rho^{\text{out}}(r) = \frac{1}{4\pi} \sum_{n,l} 2(2l+1) f_{n,l} \frac{|u_{n,l}(r)|^2}{r^2}. \tag{3.31}$$

The coefficients $0 \leq f_{n,l} \leq 1$ represent the occupation fraction of the eigenfunction with quantum numbers n and l. The factor 2 in Eq. (3.31) takes into account the spin degeneracy and $(2l+1)$ compensates for the degeneracy in the quantum number $m = -l, -l+1, ..., l-1, l$, where $l > 0$. More detail about the quantum number is given in Appendix A.3. Because it is the radial electron density, a division by $(4\pi r^2)$ is performed. Equations (3.30) and (3.31) together define a non-linear map [15];

$$K : L^1(\mathbb{R}) \to L^1(\mathbb{R}); \tag{3.32}$$

$$K[\rho^{\text{in}}] = \rho^{\text{out}}. \tag{3.33}$$

To investigate existence of solutions of the non-linear map K we state the Banach fixed-point theorem.

Theorem 2 (**Banach**). *For X a Banach space, let $\mathcal{B} : X \to X$ be a nonlinear mapping satisfying:*

$$||\mathcal{B}(u) - \mathcal{B}(w)|| \leq \gamma ||u - w|| \qquad \forall u, w \in X. \tag{3.34}$$

for $\gamma < 1$. Then $\mathcal{B}$ has exactly one fixed point.

If the Kohn–Sham map K with the L^2-norm satisfies Theorem 2 locally around the initial density, we have exactly one solution. In general this is not the case for the map K. Still, we aim for a process to find an approximation to the fixed point $\rho^*(r)$ of this map, which may not be unique, such that $K[\rho^*(r)] = \rho^*(r)$. To do so, we construct a sequence $\{\rho_1^{\text{in}}, \rho_2^{\text{in}}, ..., \rho_k^{\text{in}}\}$ with $k \in \mathbb{Z}$ and introduce the fixed-point iteration:

$$\rho_{i+1}^{\text{in}} := \rho_i^{\text{out}} = K[\rho_i^{\text{in}}]. \tag{3.35}$$

The stopping criterion is based on the total energy, once this has the acquired accuracy, denoted by the accuracy paramter ε, the sequence can be ended. The total energies are calculated by (3.20) and once $|E_{i+1}^{\text{in}} - E_i^{\text{in}}| < \varepsilon$ for some $\varepsilon > 0$ the SCF loops stops and convergence is achieved. Instead of (3.35), we introduce a new fixed point iteration with linear admixing:

$$\rho_{i+1}^{\text{in}} = (1-\kappa)\rho_i^{\text{in}} + \kappa K[\rho_i^{\text{in}}], \quad \kappa \in (0, 1]. \tag{3.36}$$

It is proven that for the fixed-point iteration presented in (3.36), assuming that the map K is non-expansive ($\gamma = 1$), there always exist a κ such that the iteration converges [16]. It is typically assumed that the map K is non-expansive. Based on the linearly admixed fixed-point iteration, the implemented SCF process is described with use of a flowchart. The initial density we use is described by the function:

$$\rho^{\mathrm{in}}(r) = \frac{N^4}{64\pi} e^{-pr/2}. \tag{3.37}$$

It can be checked $N = \int_0^\infty r^2 \rho^{\mathrm{in}}(r)\mathrm{d}r$. The initial density thus agrees with the number of particles.

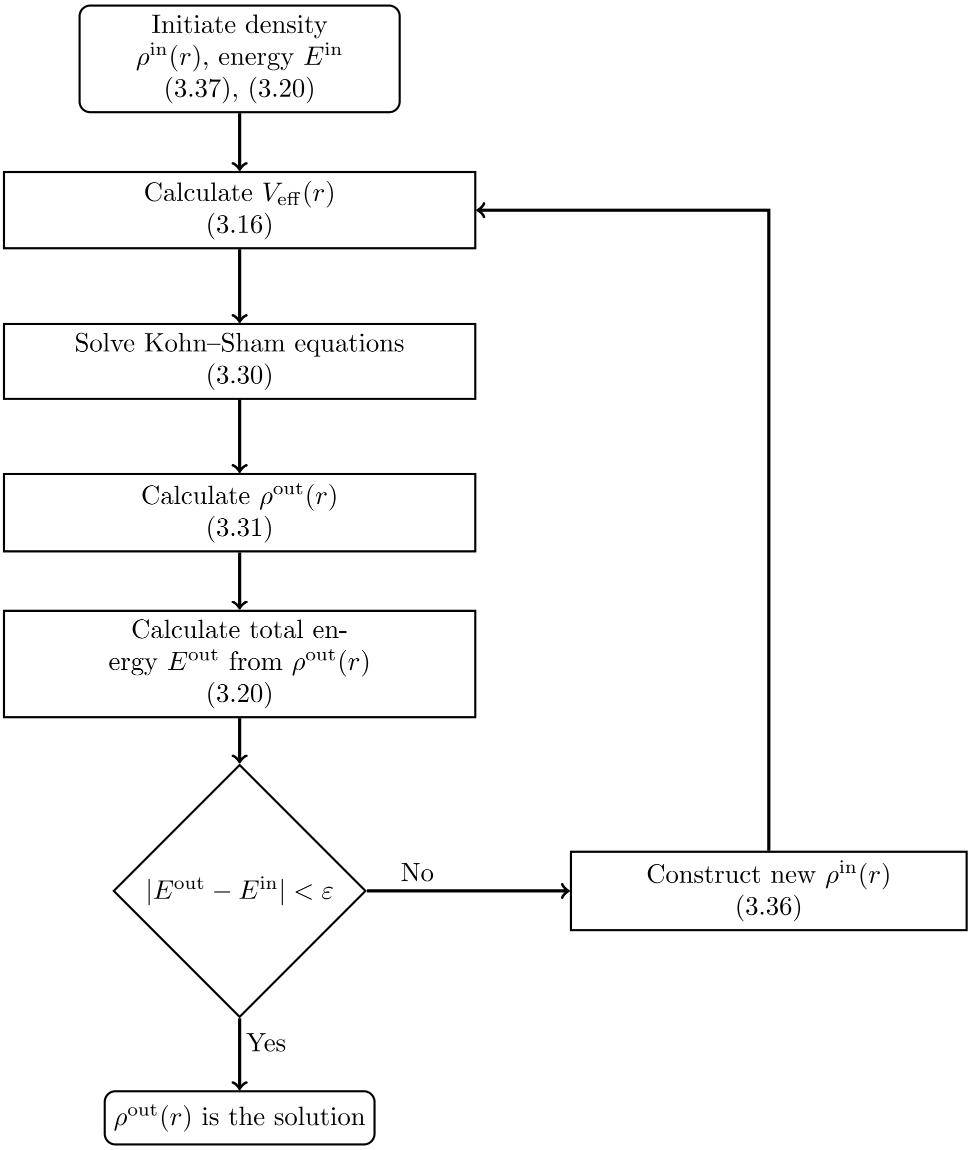

Figure 3.1: Flowchart for the solution method of the self-consistent Kohn–Sham equations.

Chapter 4

Results and discussion

In this chapter, the results of the LDA and LDAq algorithm will be shown and discussed. We start with Hydrogen and standard LDA, where $q = 4/3$. The total energies, Kohn–Sham potential and radial wavefunctions are compared to the analytical solution to test the accuracy and correctness of the numerical method. Next, the total energies for atoms up till atomic number $Z = 10$ are calculated with standard LDA and compared to known values. After that, the generalised local-density approximation is analysed for two extreme cases and the intermediate regime around $q = 4/3$. The ionisation energy, total energy as well as the wave functions will be covered.

4.1 Standard LDA

We run the DFT calculation for Hydrogen and compare it to the exact solution. The accuracy parameter of the SCF-loop is set at $\epsilon = 1e-5$ Hartree. Convergence of the solutions was achieved in 35 iterations of the SCF-loop. A plot of the various contributions to the Kohn–Sham potential and the radial probability is given in Fig. 4.1 and Fig. 4.2.

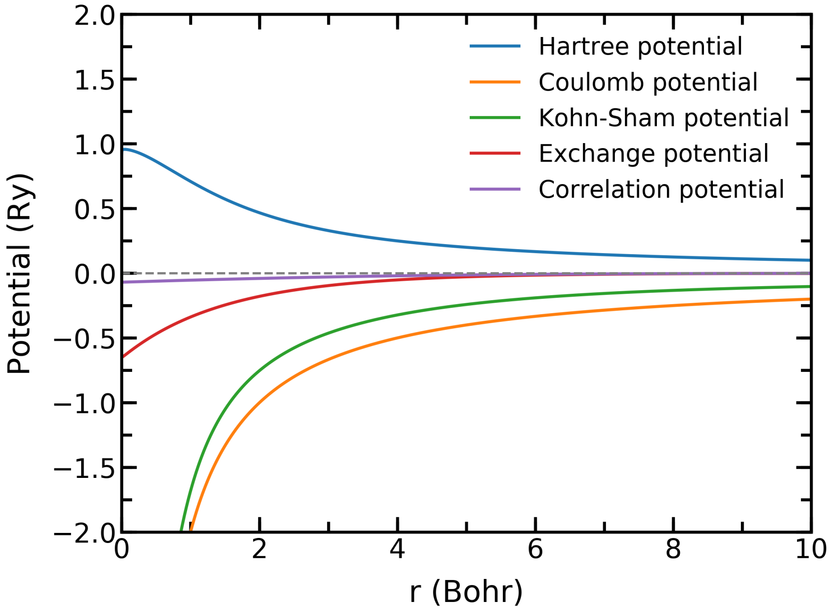

Figure 4.1: Kohn–Sham potential together with its components, Hartree, Coulomb, exchange and correlation potential shown against radial distance r for Hydrogen atom.

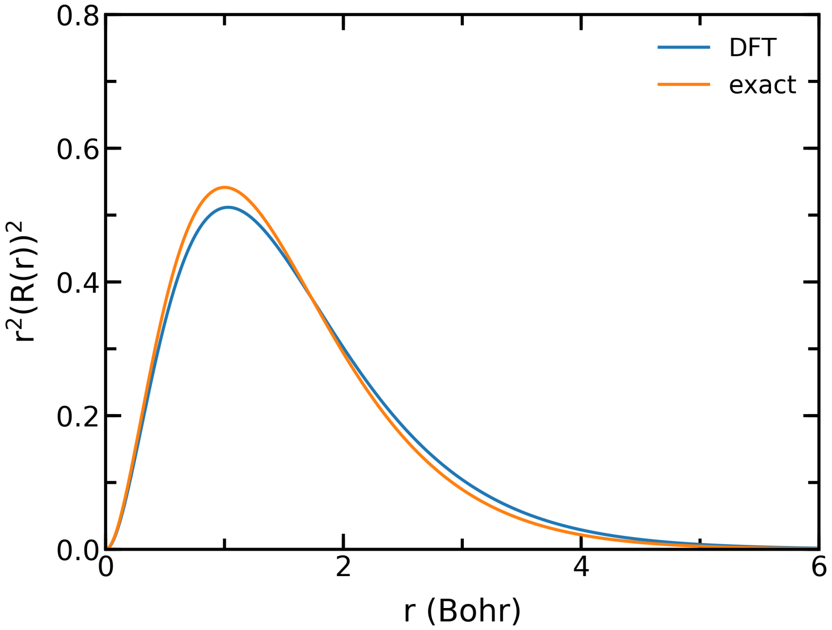

Figure 4.2: Radial probability $r^2(R(r))^2$ as function of the radial distance r for the DFT calculation compared against the exact solution for Hydrogen atom.

From Fig. 4.1, it can be seen that the Hartree potential does not quite cancel with the exchange-correlation potential through which the self-interaction becomes apparent. As a result the Kohn-Sham potential is slightly above the Coulomb potential, which indicates that the bound states will shift up with respect to the analytical ground state energy of Hydrogen (-0.5 Hartree) that corresponds to the Coulomb potential. The LDA calculation predicts a ground state of -0.4456 Hartree, which is in line with our intuition. A plot of the radial probability distribution for the LDA calculation is given in Fig. 4.2, together with the exact result. The LDA calculation gives a result slightly different from the exact result, which is expected as the calculated ground state energy is higher. The weight in the radial probability is shifted to the right for the LDA calculation with respect to the analytical result. This can be explained by the erroneous self-interaction which is repulsive.

The total binding energy for atoms up to and including $Z = 10$ is predicted by LDA. The results are summarized in Table 4.1 in the column LDA and compared to experimentally known values.

Atom	Z	Experiment[1]	LDA
H	1	-0.5 [2]	-0.4456
He	2	-2.9034	-2.8504
Be	4	-14.7833	-14.5349
C	6	-37.8558	-37.6305
Ne	10	-129.054	-129.0547 [3]

[1] Energies retrieved from NIST database [17]

[2] Exact energy [4]

[3] Parameters ($N = 1200, r_{\text{max}} = 45, \kappa = 0.4$)

Table 4.1: Total energies E_{tot} in Hartree units, comparison between values known from theory and experiment and LDA result. Used parameters: ($N = 1000, r_{\text{max}} = 60, \kappa = 0.4$)

4.2 Generalized local-density approximation

We analyze results by using the generalization of the exchange energy in LDAq given by (2.44) For Hydrogen, we establish two limiting cases, the first one is $q \downarrow 1$ and the second limit is $q \to \infty$. After that the intermediate regime is treated for various atoms in the periodic table and different q-values which includes the physical value $q = \frac{4}{3}$ in the HEG. Since we are mainly interested in the scaling with q, we take $\lambda = \lambda_{\text{HEG}} = \left(\frac{3}{\pi}\right)^{1/3}$. A different constant λ would scale the exchange potential by a constant. We plot the potentials of the LDA output for $q = 1.03$ and $q = 7/2$ in Fig. 4.3a and Fig. 4.3b. These give us an idea of what happens in both limiting cases. The results are shown without correlation potential.

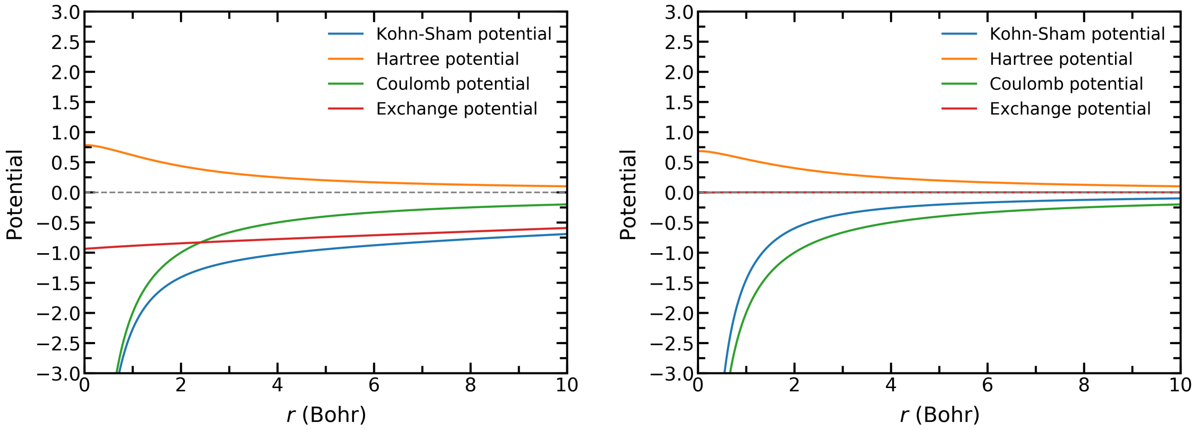

(a) $q = 1.03$.

(b) $q = 7/2$

Figure 4.3: Kohn–Sham potential together with its components, Hartree, Coulomb, exchange potential shown against radial distance r for Hydrogen atom

Upon taking the limit $q \downarrow 1$, the exchange potential is given by:

$$V_{\mathrm{x}}[\rho(\mathbf{r})] = -\lim_{q \downarrow 1} \lambda \rho(\mathbf{r})^{q-1} = -\lambda. \tag{4.1}$$

Now take the limit $q \to \infty$, then the exchange potential is given by:

$$V_{\mathrm{x}}[\rho(\mathbf{r})] = -\lim_{q \to \infty} \lambda \rho(\mathbf{r})^{q-1} = 0. \tag{4.2}$$

For both cases, set $V_{\mathrm{c}}[\rho(\mathbf{r})] = 0$. These limiting cases agree with our numerical output in Fig. 4.3a and Fig. 4.3b. Upon choosing q smaller or bigger, the exchange potential becomes constant in both cases. The resulting equations we get for both system can be combined into a single equation:

$$\left[-\frac{1}{2}\nabla^2 - \frac{Z}{r} + \int_{\mathbb{R}^3} \mathrm{d}\mathbf{r}' \frac{\rho(\mathbf{r}')}{|\mathbf{r}-\mathbf{r}'|} + c \right] \phi_i(\mathbf{r}) = \epsilon_i \phi_i(\mathbf{r}). \tag{4.3}$$

The constant $c \in \{-\lambda, 0\}$ corresponds to the limit $q \downarrow 1$ or $q \to \infty$. Equations (4.3) are the Hartree–Fock equations (2.27) where the exchange term is set to 0. In the case $c = -\lambda$, a constant is added to the Hartree equations. In principle, the difference in the eigenvalues would thus be different by this constant λ. We numerically check convergence of the eigenvalues in both limits by choosing q-values slightly above 1 and large q-values. Next to that, we can set the exchange potential to the values $-\lambda$ and 0 respectively, which corresponds to taking the limit. The difference between the eigenvalues of both limits is calculated to be 0.947. This is slightly off with respect to the constant $\lambda = \left(\frac{3}{\pi}\right)^{1/3} \approx 0.985$. Theoretically, the constant c cannot change the eigenfunctions, the reason why the eigenvalues do not converge to the exact constant λ is likely due to numerical artefacts. These may include the finite $r_{\max}$ and number of points N.

We remark that in the LDAq algorithm, taking the limits $q \downarrow 1$ and $q \to \infty$ results in the same system, apart from a constant $-\lambda$. In both cases, the exchange interaction is not a functional anymore. In between both limits, the physical value $q = \frac{4}{3}$ lies and we have the local-density approximation.

4.3 Intermediate regime

We have seen that the two limits for q are connected and basically equivalent, up to a constant. Now we want to turn our focus on the intermediate regime, which for our purposes is a region around $q = \frac{4}{3}$ represented by $1.1 \leq q \leq 1.6$. Between the two limits (Sec. 4.2), the Kohn–Sham potential shifts from below the Coulomb potential to finally above the Coulomb potential. Somewhere in the intermediate regime, the LDAq algorithm gives a prediction for the total energy which equals the real experimentally known value. To investigate what q value is optimal given an atomic number Z, a heat map is made. For a range of values q, the total energy output of the LDAq algorithm is divided by the experimentally known values [17]. From the ratio, the optimal q value can be obtained and made visual. Theoretically, the optimal ratio is 1. we cannot achieve this exactly with LDAq, but aim for a ratio close to 1.

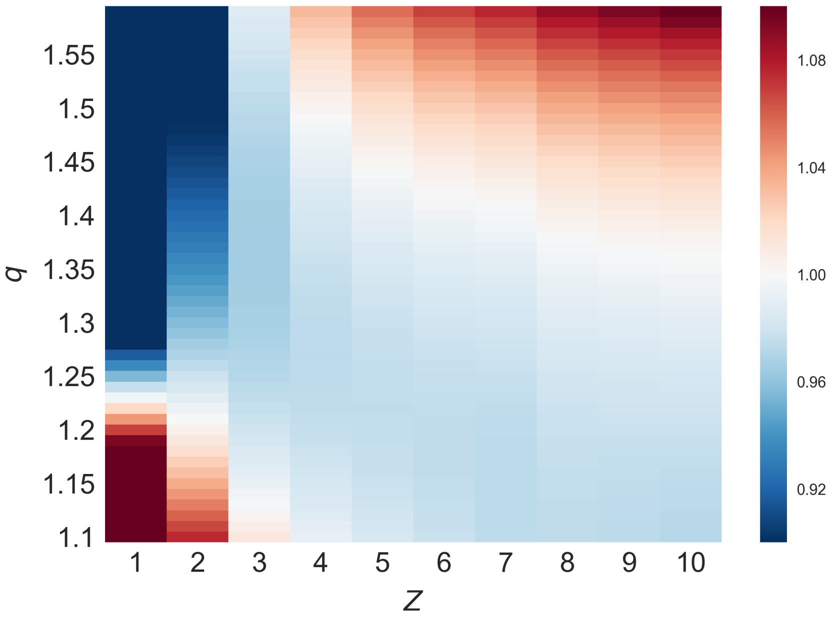

Figure 4.4: Heat map representing the ratio $\frac{E_{\text{tot}}}{E_{\text{exp}}}$ for a range of q values and atomic numbers Z

From Fig. 4.4 it becomes apparent that for larger atomic numbers near $Z = 10$, the ratio is close to 1 around $q = \frac{4}{3}$, based on the HEG. The system with more electrons might behave more uniform, which would explain why it is better resembled by the homogeneous electron gas. For Hydrogen ($Z = 1$), the prediction is quite bad in comparison to bigger atoms. This is due to the self-interaction which induces the biggest error in Hydrogen as it only consists of one electron. The ratio of the total energy does, however, not give the full picture. Suppose we tune our q such that the prediction of the LDAq algorithm is close to the optimal for a fixed Z. The total energy is then calculated with high precision, but other properties might be lost. Based on Janak's theorem, the ionisation energy $I(Z)$ can be related to the highest occupied Kohn–Sham orbital eigenenergy [18]. It follow from Janak's theorem that

$$-\epsilon_{\max}(N) = I(Z), \tag{4.4}$$

where $\epsilon_{\max(N)}$ is the highest occupied Kohn–Sham eigenenergy. Our LDAq algorithm calculates all orbital eigenenergies, which can again be compared with theoretical and/or experimentally known ionisation energies [17]. We define the ratio $-\frac{\epsilon_{\max}}{I(Z)}$ and investigate whether this ratio and the total energy ratio can be optimal at the same time. A scatter plot is made of the ratio $-\frac{\epsilon_{\max}}{I(Z)}$ against $\frac{E_{\text{tot}}}{E_{\text{exp}}}$, with and without correlation potential for $Z = 4$ and $Z = 10$. Here, the theoretical optimum is the point $(1, 1)$. It is however not clear if we can approach this optimum where both ratios equal 1. For numerical purposes, we define optimal as having the smallest Euclidian distance between the points $(-\frac{\epsilon_{\max}}{I(Z)}, \frac{E_{\text{tot}}}{E_{\text{exp}}})$ and $(1, 1)$.

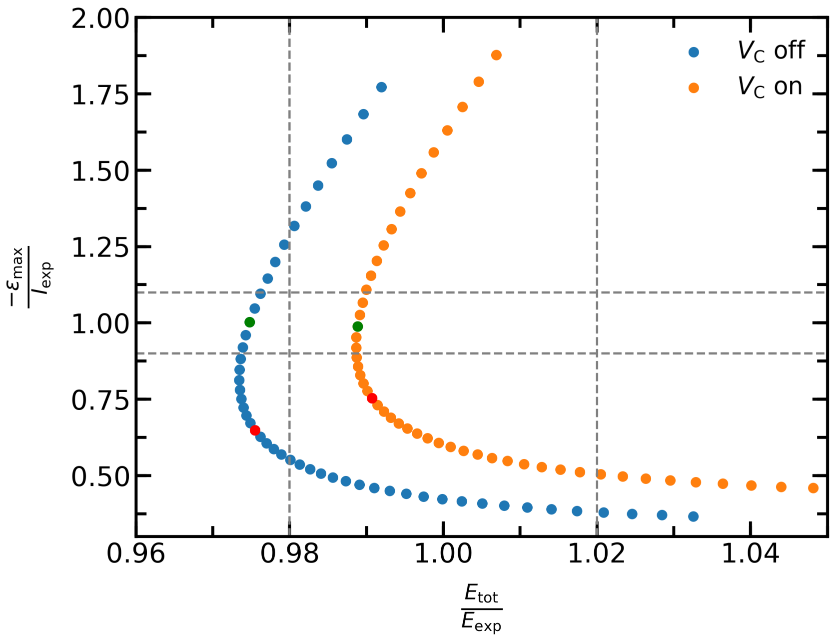

Figure 4.5: Scatter plot of the ratio $-\frac{\epsilon_{\max}}{I(Z)}$ against $\frac{E_{\mathrm{tot}}}{E_{\exp}}$ for atomic number $Z = 4$, with and without correlation potential. Each point corresponds to a different $q \in \{1.1, ...1.6\}$

In Fig. 4.5, $q = 4/3$ value is marked by the red dot. The optimal point is marked green and is attained at a value 1.22 when the correlation potential is turned off and $q = 1.25$ with the correlation potential turned on. We are interested in a region where both the ionisation energy and the total energy are close to experimentally known values. This is made visual by the dotted straight lines. Including the correlation potential, there exist values of q for which $0.9 < \frac{\epsilon_{\max}}{I(Z)} < 1.1$ and $0.98 < \frac{E_{\mathrm{tot}}}{E_{\exp}} < 1.02$ at the same time. When the correlation potential is turned off, the accuracy decreases as the distance between predicted ratios and the optimal point becomes larger. In this framework, the accuracy of different correlation potentials could also be investigated. Notice that the error in the ionisation energy ratio is typically larger than the total energy ratio. Because of this, a small decrease in accuracy in the total energy ratio can result in a big improvement for the ionisation energy ratio, which is visualised in the curves. Also, we remark that the total energy ratio has two optima where the ratio becomes one, in the case where $Z = 3$ or $Z = 4$. This was already concluded from the heat map in Fig. 4.4. A similar scatter plot is made for $Z = 10$.

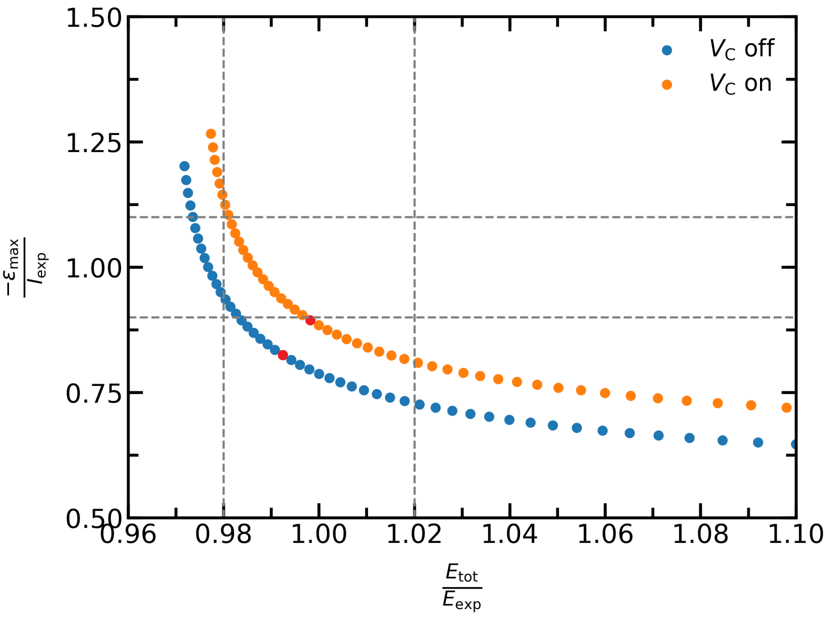

Figure 4.6: Scatter plot of the ratio $-\frac{\epsilon_{\max}}{I(Z)}$ against $\frac{E_{\mathrm{tot}}}{E_{\exp}}$ for atomic number $Z = 10$, with and without correlation potential. Each point corresponds to a different $q \in \{1.1, ...1.6\}$

In Fig. 4.6, the points corresponding to the physical value $q = \frac{4}{3}$ are again marked by the red dot. For larger total energy ratios, the dots are separated by a difference $\Delta q = 0.01$ up until $q = 1.6$. For smaller total energy ratios, q decreases in steps Δq towards $q = 1.1$. For $Z = 4$, we observed that there were two optimal solutions. This is not the case anymore for larger Z. For smaller values $q = 1.01$, the total energy ratio without correlation potential was 0.969. The blue dots in Fig. 4.6 tends to an asymptote around the total energy ratio at the value 0.969 for $q \downarrow 1$. It would be interesting to know whether there exists a correlation potential with goes through the optimal point $(1, 1)$. If so, what does this say about the physical properties and how does this behaviour change with respect to the atomic number Z? We also observe that the curves in Fig. 4.5 and Fig. 4.6 look to be symmetric with respect to straight line with some positive slope.

4.3.1 Norms

The purpose of this section is to check whether assumptions made in [9] are physical. There, it is proven that a system consisting of the time dependent Kohn–Sham equations coupled with nuclear dynamics has a unique solution for $q \geq \frac{7}{2}$, $\lambda \in \mathbb{R}$ and some time $\tau > 0$, where the Kohn–Sham orbitals $\phi_n \in C^0([0, \tau], H^2(\mathbb{R}^3; \mathbb{C}))$. For further details of this theorem and proof, we refer to [9]. In contrast, we consider the time-independent Kohn–Sham equations and can only make statements for a fixed time. We numerically check whether the obtained solutions of the LDAq algorithm agree with the initial assumption at $t = 0$ by checking the L^2, H^1 and H^2 norms of the first Kohn–Sham eigenfunction ϕ_1 for various q. If a blow-up occurs, this might indicate the assumptions are too strict. If not, the assumptions are like to be realistic at $t = 0$ by numerical validation, no statement about later times can be made though. The norms are calculated from the radial Kohn–Sham eigenfunctions using spherical symmetry:

$$||\phi_1||_{L^2}^2 = \int_{\mathbb{R}_{\geq 0}} \mathrm{d}r 4\pi r^2 \phi_1^*(r)\phi_1(r). \tag{4.5}$$

The H^1- and H^2-norms are calculated using the definitions (A.7) and (A.8), again using spherical symmetry and multiplying by $4\pi r^2$.

Z	q	$\|\|\phi_1\|\|_{L^2}$	$\|\|\phi_1\|\|_{H^1}$	$\|\|\phi_1\|\|_{H^2}$
1	1.03	1.0	1.60	1.89
1	4/3	1.0	1.68	2.10
1	7/2	1.0	1.53	1.77
1	10000	1.0	1.54	1.77

Table 4.2: Calculation of the L^2-, H^1- and H^2-norms for different q values.

All the norms are bounded and no blow-up phenomenon is encountered. Also, the L^2-norm evaluates to 1 for a single-electron orbital, as should be due to normalisation.

Chapter 5

Conclusion

The goal of this thesis was to investigate the physical properties of a generalised local-density approximation in density-functional theory. The developed LDA code gives results for the total energy that is in good agreement with known theoretical and experimental results. The self-interaction remains a problem, which is the biggest issue for Hydrogen, for which the predicted total energy is 10% higher. For $Z \in \{2, ..., 10\}$, total energies are within 2% accuracy. Convergence of the self-consistent loop was usually achieved within 50 iterations.

The generalisation of the exchange interaction depending on the parameter $q > 1$ and constant $\lambda \in \mathbb{R}$ is captured in the LDAq code. When the correlation term is set to 0 and in the limit where $q \downarrow 1$ and $q \to \infty$, the Kohn–Sham equations reduced to the Hartree equations, with and without an additional constant $-\lambda$ respectively. It was also checked numerically that the exchange potential converges to a constant in both limiting cases. Although the Kohn–Sham equations and the Hartree equations are derived from different assumptions, a connection between both can be made. For intermediate q-values, we arrive back at the local-density approximation.

From the analysis of the homogeneous electron gas we know that the physical value is $q = \frac{4}{3}$. For other non-homogeneous systems, like atoms, there is no exact value for q. A better prediction might result from a different choice of the parameter q. To investigate this, for 60 q-values between 1.1 and 1.6, the LDAq algorithm's output is divided by the theoretically or experimentally known total energy. The resulting ratio is visualized in a heat map for q against atoms number $Z \in \{1, ..., 10\}$. We conclude that for Z approaching 10 in integer steps, the optimal ratio ($= 1$) is attained for values of q approaching $\frac{4}{3}$ from above. For larger Z, the density might becomes more and more uniform, therefore the homogeneous electron gas value $q = \frac{4}{3}$ better describes the atomic system. For $Z = 1$ and $Z = 2$, the optimal ratio is taken at a value $q = 1.23$ and $q = 1.21$ respectively. This results from the erroneous self-interaction, which is most apparent in Hydrogen and Helium. Via the heat map, an optimal q-value can be chosen so that the total energy is approximated in a best possible way, after which extrapolation methods might predict results for higher values of Z. To see if this is useful, we must make sure that other properties are not destroyed by scanning over q. Via Janak's theorem, the ionisation energy is linked to the highest occupied Kohn–Sham eigenenergies. This defines an ionisation energy ratio, which is visualised in a scatter plot against the total energy ratio. There is a trade-off between the accuracy in the total energy and the ionisation energy. A small decrease in accuracy of the total energy ratio around 1% can lead to a big increase in the ionisation energy ratio of at least 10%. We propose that a better correlation potential might shift results closer to the theoretical optima where both ratios equal 1.

Several norms have been calculated for various q, i.e. the L^2-, H^1- and H^2-norms. All norms remain finite and no blow-up phenomena is observed. The assumptions for the single-electron orbitals being in the corresponding spaces thus seem valid.

Bibliography

[1] Jianwei Sun, James W. Furness, and Yubo Zhang. Density functional theory. *Mathematical Physics in Theoretical Chemistry*, pages 119–159, 1 2019.

[2] Stephen J. Gustafson and Israel Michael Sigal. *Mathematical Concepts of Quantum Mechanics.* Universitext. Springer Berlin Heidelberg, Berlin, Heidelberg, 2011.

[3] Jos Thijssen. The Hartree–Fock method. *Computational Physics*, pages 43–88, 2007.

[4] David J. Griffiths and Darrell F. Schroeter. *Introduction to quantum mechanics.* Cambridge University Press, third edition, 2018.

[5] P. Hohenberg and W. Kohn. Inhomogeneous electron gas. *Physical Review*, 136(3B):864–871, 1964.

[6] Eberhard Engel and Reiner M. Dreizler. *Density Functional Theory.* Theoretical and Mathematical Physics. Springer Berlin, Heidelberg, first edition, 2011.

[7] W. Kohn and L. J. Sham. Self-consistent equations including exchange and correlation effects. *Physical Review*, 140(4A):A1133, 1965.

[8] W Kohn. Nobel Lecture: Electronic structure of matter-wave functions and density functionals. *Rev. Mod. Phys*, 71:1253–1266, 1999.

[9] Björn Baumeier, Onur Çaylak, Carlo Mercuri, Mark Peletier, Georg Prokert, and Wouter Scharpach. Existence and uniqueness of solutions to the time-dependent Kohn-Sham equations coupled with classical nuclear dynamics, 2020. arXiv:2011.10542 [math.AP].

[10] S. H. Vosko and L. Wilk. Influence of an improved local-spin-density correlation-energy functional on the cohesive energy of alkali metals. *Physical Review B*, 22(8):3812, 1980.

[11] Jay S Bolemon. Computer Solutions to a Realistic 'One-Dimensional' Schrödinger Equation. *American Journal of Physics*, 40:1511, 1972.

[12] Nathalie Holzwarth. Numerical methods of solving Kohn-Sham equations for atoms, 2011.

[13] Witold A. J. Kosmala. *A friendly introduction to analysis.* Pearson Prentice Hall, second edition, 2004.

[14] Wolfram Koch and Max C. Holthausen. *A Chemist's Guide to Density Functional Theory.* Wiley, second edition, 2001.

[15] N D Woods, M C Payne, and P J Hasnip. Computing the Self-Consistent Field in Kohn-Sham Density Functional Theory. *Journal of physics: Condensed Matter*, 31(45), 2019.

[16] Felix E. Browder. Convergence of approximants to fixed points of nonexpansive nonlinear mappings in banach spaces. *Archive for Rational Mechanics and Analysis*, 24(1):82–90, 1967.

[17] A Kramida and Yu Ralchenko. Nist atomic spectra database. National Institute of Standards and Technology, [Online]. Available: https://physics.nist.gov/asd [Thu Jul 7 2022].

[18] Manoj K Harbola. Relationship between the highest occupied Kohn-Sham orbital eigenvalue and ionization energy. *Physical Review B*, 60(7), 1999.

[19] R. K. Nesbet. Kinetic energy as a density functional. *Physical Review A*, 65(1):010502, 2002.

[20] Helmut Eschrig. *The Fundamentals of Density Functional Theory*. TEUBNER-TEXTE zur Physik. Vieweg+Teubner Verlag, Wiesbaden, 1996.

Appendix A

Concepts from quantum mechanics

A.1 Hilbert space

We consider a *vector space* $\mathcal{H}$. An *inner product space* is a vector space with a defined inner product, that is a map

$$\langle \cdot, \cdot \rangle : \mathcal{H} \times \mathcal{H} \to \mathbb{C} \tag{A.1}$$

that satisfies the properties

1. linearity in the second argument:
$$\langle v, \alpha w + \beta z \rangle = \alpha \langle v, w \rangle + \beta \langle v, z \rangle$$
2. conjugate symmetry: $\langle w, v \rangle = \langle v, w \rangle^*$
3. positive definiteness: $\langle v, v \rangle > 0$ for $v \neq 0$

for any $v, w, z \in \mathcal{H}$ and $\alpha, \beta \in \mathbb{C}$. This inner product defines a norm on $\mathcal{H}$ given by the map $|| \cdot || : \mathcal{H} \to [0, \infty)$ where

$$||v|| = \langle v, v \rangle^{1/2} . \tag{A.2}$$

If the inner product space is complete with respect to the introduced norm, then $\mathcal{H}$ is a Hilbert space. The phase space in quantum mechanics is always a Hilbert space. One example of a Hilbert spaces that we will use are the L^2-space:

$$L^2(\mathbb{R}^d) = \{\psi : \mathbb{R}^d \to \mathbb{C} | \int_{\mathbb{R}^d} |\psi|^2 \leq \infty\}. \tag{A.3}$$

The inner product that makes this a Hilbert space is

$$\langle \psi, \phi \rangle_{L^2} = \int_{\mathbb{R}^d} \psi^*(\mathbf{x}) \phi(\mathbf{x}) \mathrm{d}\mathbf{x}, \tag{A.4}$$

with $\mathbf{x} \in \mathbb{R}^d$ and $\psi, \phi \in L^2(\mathbb{R}^d)$. We use the notation $||\psi||_{L^2}$ to denote the L^2-norm with respect to the inner product in (A.4).

Another example of a Hilbert space is the Sobolev space of order n, $n = 1, 2, 3, ...$, which is defined as:

$$H^n(\mathbb{R}^d) = \{\psi \in L^2(\mathbb{R}^d) \quad | \quad \partial^\alpha \psi \in L^2(\mathbb{R}^d) \quad \forall \alpha, |\alpha| \leq n\}. \tag{A.5}$$

Here, the index α is a multi-index $\alpha = (\alpha_1, ..., \alpha_d)$, consisting of non-negative integers where $|\alpha| = \sum_{i=1}^d \alpha_i$. The term ∂^α can be written out using the multi-indices to $\partial_{x_1}^{\alpha_1} \cdots \partial_{x_d}^{\alpha_d}$ where $\partial_{x_1}^{\alpha_1} = \frac{\partial^{\alpha_1}}{\partial x_1^{\alpha_1}}$. The Sobolev space $H^n(\mathbb{R}^d)$ is the functional space where all derivatives up to order n lie in $L^2(\mathbb{R}^d)$. The inner product defined on this space is:

$$\langle \psi, \phi \rangle_{H^n} = \sum_{0 \leq |\alpha| \leq n} \langle \partial^\alpha \psi, \partial^\alpha \phi \rangle_{L^2}, \tag{A.6}$$

for $\psi, \phi \in H^n(\mathbb{R}^d)$. In this thesis we will work with $H^1 = H^1(\mathbb{R}^d)$ and $H^2 = H^2(\mathbb{R}^d)$, which have corresponding norms

$$||\psi||_{H^1} = \sqrt{||\psi||_{L^2}^2 + ||\nabla \psi||_{L^2}^2}, \tag{A.7}$$

$$||\psi||_{H^2} = \sqrt{||\psi||_{L^2}^2 + ||\nabla^2 \psi||_{L^2}^2}. \tag{A.8}$$

The wave functions are normalised in the L^2-norm to 1 in order to be interpreted as a probability distribution.

A.2 Schrödinger equation

The goal in quantum mechanics is to find the wave functions that govern the motion of particles in space and time. It is denoted by $\psi(\mathbf{x}, t)$, for $\mathbf{x} \in \mathbb{R}^3$ and $t \in \mathbb{R}$ denoting the position and time coordinates respectively. It must satisfy the Schrödinger equation [2]:

$$i\hbar \frac{\partial}{\partial t} \psi = H\psi, \tag{A.9}$$

where the right-hand side is the Hamiltonian operator given by

$$H\psi = -\frac{\hbar^2}{2m} \nabla^2 \psi + V\psi. \tag{A.10}$$

The constant m denotes the mass of the particle and $\hbar$ is Planck's constant. It is a fundamental constant in nature, its value is $\hbar = 1.054571817 \cdot 10^{-34}$ Js. Given suitable initial conditions, for example $\psi(\mathbf{x}, 0)$, the Schrödinger equation determines the motion $\psi(\mathbf{x}, t)$ for all $t \in \mathbb{R}^+$. The state space for the wave functions is the space of square-integrable functions over $\mathbf{x} \in \mathbb{R}^3$:

$$L^2(\mathbb{R}^3) := \{\psi : \mathbb{R}^3 \to \mathbb{C} | \int_{\mathbb{R}^3} |\psi(\mathbf{x})|^2 d\mathbf{x} < \infty\}. \tag{A.11}$$

The wave functions need to satisfy A.11 for $|\psi(\mathbf{x},t)|^2$ to be interpreted as a probability distribution. Once we have a normalised solution, it must stay normalised in time. For this, the Hamiltonian operator H must be *self-adjoint*. This important property is captured in the next theorem.

Theorem 3. *Consider the initial value problem A.9 together with the initial condition $\psi_0 \in L^2(\mathbb{R}^3)$. Solutions $\psi(t) \in D(H)$ conserve probability if and only if H is self-adjoint.*

Proof. Suppose $\psi(t) \in D(H)$ solves the initial value problem A.9 with ψ_0. Compute

$$\frac{\mathrm{d}}{\mathrm{d}t}\langle\psi,\psi\rangle = \left\langle\dot{\psi},\psi\right\rangle + \left\langle\psi,\dot{\psi}\right\rangle = \left\langle\frac{1}{i\hbar}H\psi,\psi\right\rangle + \left\langle\psi,\frac{1}{i\hbar}H\psi\right\rangle \tag{A.12}$$

$$= \frac{1}{i\hbar}\left[\langle\psi,H\psi\rangle - \langle H\psi,\psi\rangle\right] = 0. \tag{A.13}$$

In the last step we have used self-adjointness of the Hamiltonian operator. The probability distribution is thus conserved in time. □

A.3 Time-independent Schrödinger equation

For a general time-independent potential V, the Schrödinger equation (A.9) can be solved by separation of variables leading to the *time-independent Schrödinger equation*:

$$\frac{\hbar^2}{2m}\nabla^2 + V\psi = E\psi, \tag{A.14}$$

where $\psi = \psi(\mathbf{x})$ with $\mathbf{x} \in \mathbb{R}^3$. From now on, we drop the time dependence in the wave function ψ. If wanted, it can be added by multiplying with a factor $e^{-iEt/\hbar}$. Throughout this thesis, we solve (A.14) for time-independent potentials. Furthermore, we assume *central potentials*, where $V(\mathbf{x}) = V(|\mathbf{x}|)$. Adopting spherical coordinates (r,θ,ϕ), we look for solutions $\psi(r,\theta,\phi) = R(r)Y(\theta,\phi)$ such that Equation (A.14) splits in a radial wave equation and an angular equation. The discrete solutions are label by the three quantum numbers n, l and m. The quantum number n determines the energy of the state, l and m relate to the angular momentum. In terms of the function $u(r) := rR(r)$, the radial equation reads [4]

$$-\frac{1}{2}\frac{d^2u}{dr^2} + \left[V + \frac{l(l+1)}{2r^2}\right]u = Eu. \tag{A.15}$$

The electrons are subject to Pauli exclusion principle, which states that identical electrons cannot occupy the same state given by the quantum numbers (n,l,m). We consider a system of spin-free identical electrons and do not take into account spin. Because electrons can have spin up or spin down, 2 electrons can occupy the same quantum state (spin degeneracy). The electronic shells are filled according to the periodic table. For a given n, the quantum number l can take the possible values $l = 0, 1, ..., n-1$. For each l, the degeneracy in m accounts for another $2l+1$ possibilities. As an example, take Neon which has atomic number $Z = 10$ and is surrounded by 10 electrons. The $n = 1$ shell gives room for two electrons, for $n = 2$ we can have both $l = 0$ and $l = 1$. Again two electrons occupy the $n = 2$ shell with $l = 0$, but another 6 electrons have quantum number $l = 1$, after which the second shell is filled.

A.4 Functional derivatives

There exist two kinds of functional derivatives, the Fréchet and Gâteaux derivative. The Fréchet derivative is a generalisation of the total derivative in functional analysis. We are mainly interested in the

Gâteaux derivative, which is a generalisation of a partial derivative, because the derivative in density-functional theory is a Gâteaux derivative [19]. Consider two complete normed vector spaces (i.e. Banach spaces) X and Y and functional $F : X \to Y$. If there exists a linear functional $F'[x_0] \in X$, $x_0 \in X$, such that

$$\lim_{\tau \to 0} \frac{F[x_0 + \tau x] - F[x_0]}{\tau} = F'[x_0] \quad \text{for all} \quad x \in X, \tag{A.16}$$

with scalar τ, then $F'[x_0]$ is called the Gâteaux derivative of F at x_0 [20]. A Hilbert space is an example for a Banach space. In our case, we work with a specific Hilbert space and set $X = Y = L^2(\mathbb{R}^d)$ and let $\mathbf{x} \in \mathbb{R}^d$. We denote the Gâteaux derivative also by $g(\mathbf{x})$ and introduce the short-hand notation:

$$\frac{\delta F[f]}{\delta f(\mathbf{x})} = g(\mathbf{x}), \tag{A.17}$$

which will be used throughout this thesis.